CHEMISTRY
A EUROPEAN JOURNAL

DOI: 10.1002/chem.201000143

Comparison of Thiophene–Pyrrole Oligomers with Oligothiophenes: A Joint Experimental and Theoretical Investigation of Their Structural and Spectroscopic Properties

María Moreno Oliva,[a] Ted M. Pappenfus,*[b] Jacob H. Melby,[b]
Kathryn M. Schwaderer,[b] Jared C. Johnson,[b] Kari A. McGee,[c]
Demetrio A. da Silva Filho,[d] Jean-Luc Bredas,[d] Juan Casado,*[a] and
Juan T. López Navarrete*[a]

Abstract: We have prepared a new series of mixed thiophene–pyrrole oligomers to investigate the electronic benefits arising from the combination of these two heterocycles. The oligomers are functionalized with several hexyl and aryl groups to improve both processability and chemical robustness. An analysis of their spectroscopic (absorption and emission), photophysical, electrochemical, solid state, and vibrational properties is performed in combination with quantum-chemical calculations. This analysis provides relevant information regarding the use of these materials as organic semiconductors. The balance between the high aromatic character of pyrrole and the moderate aromaticity of thiophene allows us to address the impact of the coupling of these heterocycles in conjugated systems. The data are interpreted on the basis of the aromaticity, molecular conformations, ground and excited electronic state structures, frontier orbital topologies and energies, oxidative states, and quinoidal versus aromatic competition.

Keywords: heterocycles · oligomers · oligothiophenes · quantum chemistry · semiconductors

Introduction

An important research avenue to develop new organic materials acting as semiconductors in organic electronics is the investigation of molecules addressing a variety of forms of conjugation.[1] Classic examples include acenes[2] and oligothiophenes.[1a,3] In these two groups, several strategies have been used to search for improved materials. In oligothiophenes, for instance, many chemical modifications, such as ring fusion,[4] chain-length elongation[5] (i.e., up to the 96-mer), replacement of sulfur by other heteroatoms,[6] substitution of the α-terminal and β-inner positions with alkyl and electroactive groups,[7] combination with acenes,[8] selective sulfur oxidation,[9] and so on, have been reported. In particular, incorporation of different heteroatoms targets the modification/improvement of the π-conjugation, whereas inclusion of alkyl chains at the α- and β- positions leads to processability benefits and π-stacking in the solid state.[10]

Pyrrole-based oligomers have been less intensively studied for organic device applications relative to their oligothienyl homologues.[11–13] This fact may be due, in part, to the limited synthetic routes available to oligopyrroles.[14] Recently, however, Fujii et al.[14b] have reported the use of thiophene–pyrrole mixed oligomers in organic field-effect tran-

---

[a] M. M. Oliva, Dr. J. Casado, Prof. J. T. López Navarrete
Department of Physical Chemistry
University of Málaga
Campus de Teatinos s/n, Málaga 29071 (Spain)
Fax: (+34) 952-132000
E-mail: casado@uma.es
teodomiro@uma.es

[b] Dr. T. M. Pappenfus, J. H. Melby, K. M. Schwaderer, J. C. Johnson
Division of Science and Mathematics
University of Minnesota Morris
MN 56267 (USA)
Fax: (+1) 320-589-6371
E-mail: pappe001@morris.umn.edu

[c] Dr. K. A. McGee
Department of Chemistry
University of Minnesota Minneapolis
MN 55455 (USA)

[d] Dr. D. A. da Silva Filho, Prof. J.-L. Bredas
School of Chemistry and Biochemistry
Georgia Institute of Technology
Atlanta, GA 30332-0400 (USA)

Supporting information for this article is available on the WWW under http://dx.doi.org/10.1002/chem.201000143. General synthetic considerations, new calculation data together with additional X-ray measurement details. CCDC-06127x contains the supplementary crystallographic data for **Hex2-TPT**. These data can be obtained free of charge from The Cambridge Crystallographic Data Centre via www.ccdc.cam.ac.uk/data_request/cif for are provided.

sistors (OFETs) with mobilities exceeding values of 10^{-2} cm^2 V^{-1} s^{-1}. Given the renewed interest in these materials and the fact that pyrrole–thiophene co-oligomers have not been thoroughly investigated,[11–13] our goal in this work is to shed additional light on the physical properties such oligomers exhibit.

Homogeneous oligothiophenes have been synthesized with a multitude of chemical variants for use in device applications, such as OFETs,[1,3,4,9,15] OLEDs[1,3,9,16] (organic light-emitting diodes), organic photovoltaics,[17] and optically pumped organic lasers.[18] Given this diverse spectrum of applications for the related oligothiophenes, here we report the study of a new series of thiophene–pyrrole co-oligomers (**3T**, **Hex2-3T**, **Hex2-5T**, **TPT**, **Hex2-TPT**, **Hex2-TTPTT**, **TPT-p(HP)**, **Hex2-TPT-p(HP)**, **Hex2-TTPTT-p(HP)**) with the following features: 1) The nitrogen on the pyrrole ring either carries a proton or is functionalized with an aryl group. 2) The molecules are capped with hexyl groups at the α-terminal positions to enhance both electronic and solid-state properties; such hexyl substitutions have been shown to promote favorable crystalline arrangements.[10] 3) These modifications are applied to various chain lengths and number of conjugating units in the main chain.

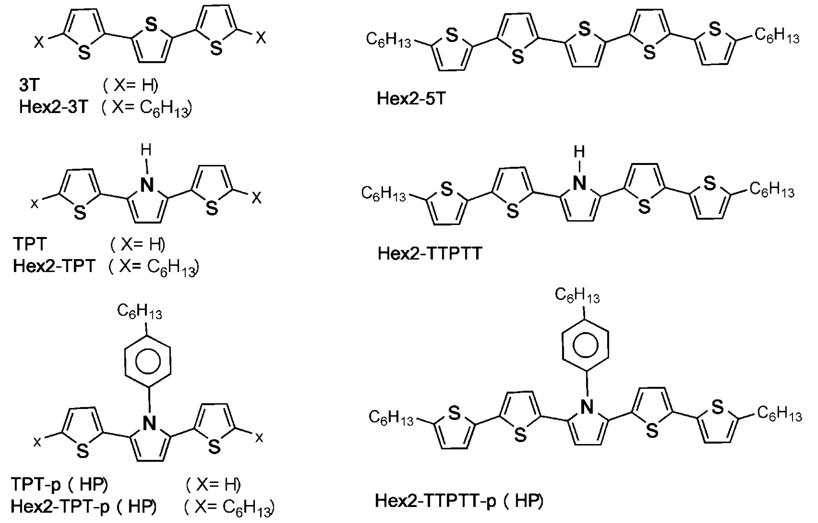

In the design of new π-conjugated molecules, one of the key parameters to optimize is the band gap, by which we define here: 1) the absolute energy difference between the HOMO and LUMO orbitals, 2) the optical gap, and 3) the electrochemical (transport) gap. These energy differences critically decide many of the electronic properties important for engineering of the semiconducting properties, such as charge injection ability, p- and n-doping (ambipolar behavior), photoluminescence, etc. In this work, we focus on some of these properties by relating the spectroscopy of these molecules in the context of the band-gap properties directly related to the linear inter-ring π-electron conjugation. The approach includes studying the electronic absorption and emission spectra, the electrochemical properties, and the vibrational Raman spectra in combination with their theoretical estimation. In all cases, we discuss in depth the comparison between the co-oligomers and the homogeneous oligothiophenes of the same length and substitution pattern. Our study includes both neutral and oxidized species. We believe that this new series of materials together with the analysis of their electronic and structural properties will be of value to the chemical community in general and the organic electronics community in particular.

Experimental Section and Theoretical Details

Synthesis: The hexyl-capped trimers were prepared according to the procedures outlined in Scheme 1. The previously reported[19] **Hex2–3T** was prepared by an alternative procedure using Stille coupling.[20] The reaction of 2,5-dibromothiophene with excess 2-hexyl-5-(tributylstannyl)thiophene afforded **Hex2–3T** in 54 % yield. Although 1,4-bis(2-thienyl)-1,4-butanedione can be prepared in high yield (> 80 %) by the Friedel–Crafts reaction,[21] preparation of analogous diketones with 2-alkyl-substituted thiophenes has been reported to proceed at much lower yields.[22] We obtained similar results for the reaction of 2-hexylthiophene with succinyl chloride to produce the targeted diketone **1** (Scheme 1). Paal–Knorr condensation[21,23] of **1** with the appropriate ammonium salt or amine afforded the desired dithienylpyrroles **Hex2-TPT** and **Hex2-TPT-(pHP)** in good yields.

The hexyl-capped pentamers were prepared according to the procedures in Scheme 2. The reaction of 1,4-bis(5-bromo-2-thienyl)-1,4-butanedione with excess 2-hexyl-5-(tributylstannyl)thiophene afforded the intermediate diketone **2** in 79 % yield. Paal–Knorr condensation of **2** with the appropriate ammonium salt or amine afforded the desired dithienylpyrroles **Hex2-TTPTT** and **Hex2-TTPTT-(pHP)** in modest yields. Dihexylquin-

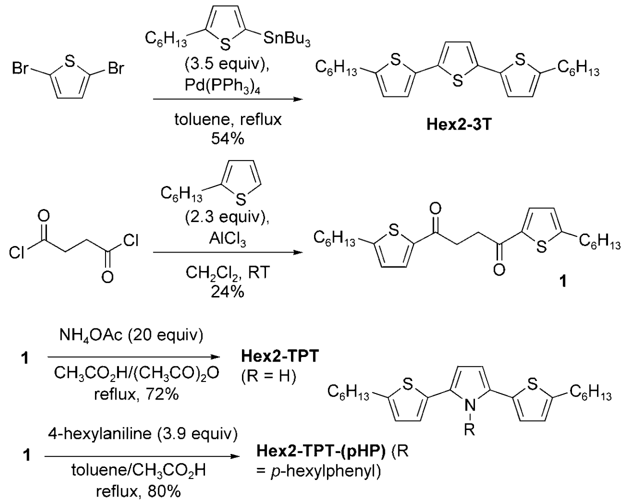

Scheme 1. Synthesis of the trimers investigated in this study.

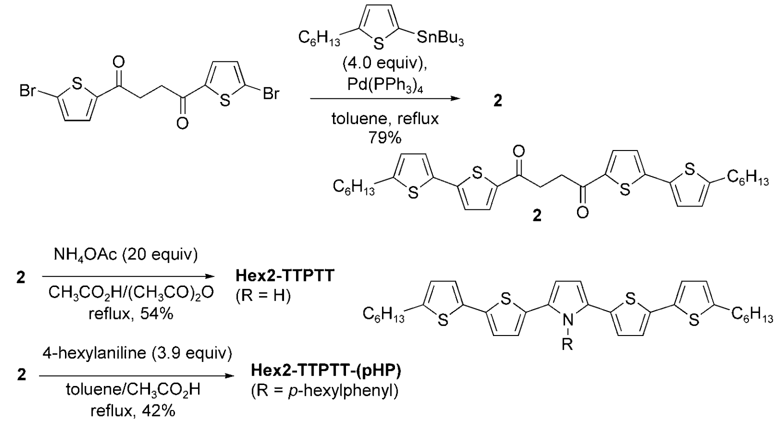

Scheme 2. Synthesis of the pentamers in this study.

quethiophene **Hex2–5T** was prepared in a similar manner as previously reported.[24] Detailed synthetic procedures and analytical data are found in the Supporting Information section of this paper.

Spectroscopic measurements: UV/Vis absorption spectra were recorded on an Agilent 8453 instrument equipped with a diode array detection system. Emission spectra were measured by using a spectrofluorimeter from Edinburgh Analytical Instruments (FLS920P) equipped with a pulsed xenon flash-lamp. Fluorescence decays were measured by using a single-photon photomultiplier detection system (S900) with picosecond pulsed diode laser (PDL 800-B), from Edinburgh Instruments. All solvents used were of spectroscopic grade from Aldrich. Fluorescence quantum yields, ϕ_F, were measured for all the solutions by using $1\times10^{-7}\,\mathrm{mol\,L^{-1}}$ quinine sulfate in $0.1\,\mathrm{mol\,L^{-1}}$ H_2SO_4 as the standard ($\phi_F=0.546$).

1064 nm FT-Raman spectra were measured by using an FT-Raman accessory kit (FRA/106-S) of a Bruker Equinox 55 FT-IR interferometer. A continuous-wave Nd-YAG laser working at 1064 nm was used for excitation along with a germanium detector operating at liquid nitrogen temperature. Raman scattering radiation was collected in a back-scattering configuration with standard spectral resolutions of 4 and $1\,\mathrm{cm^{-1}}$. 1000–3000 scans were averaged for each spectrum.

UV/Vis-NIR and Raman spectrochemistry was done by chemical oxidation by using $FeCl_3$ as the oxidant in anhydrous dichloromethane. This strong oxidizing agent was chosen according to the redox potential obtained electrochemically.

Electrochemical measurements: Room-temperature electrochemical measurements were performed with a BAS 100B electrochemical analyzer and C3 cell stand in a three-electrode configuration with a glassy carbon working electrode ($A=0.07\,\mathrm{cm^2}$), a platinum counter electrode, and a standard Ag|AgCl|KCl (1.0 M) reference electrode. A single compartment, low volume cell was used for all measurements. Tetrabutylammonium hexafluorphosphate electrolyte solution was added to the cell (5 mL, 0.1 M/CH_2Cl_2) and background cyclic voltammograms of the electrolyte solution were recorded prior to the addition of the sample. Suitable amounts of sample were added to create 0.5 mM solutions. The E^0 values for the ferrocenium/ferrocene couple for concentrations similar to those used in this study were 0.43 V for dichloromethane solutions at a glassy carbon electrode. Anodic–cathodic peak separations were typically 80–90 mV for this redox couple.

Single-crystal X-ray analysis of Hex2-TPT: Crystals of **Hex2-TPT** were grown from slow evaporation of a CH_2Cl_2/hexane solution. A crystal (approximate dimensions $0.45\times0.15\times0.10\,\mathrm{mm^3}$) was placed onto the tip of a 0.1 mm diameter glass capillary and mounted on a Siemens SMART Platform CCD diffractometer for a data collection at 173(2) K. The data collection was carried out by using $Mo_{K\alpha}$ radiation (graphite monochromator). The intensity data were corrected for absorption and decay (SADABS).[25] Final cell constants were calculated from the *xyz* centroids of 3486 strong reflections from the actual data collection after integration (SAINT).[26] The structure was solved by using SHELXS-97 (Sheldrick, 1990)[26] and refined by using SHELXL-97 (Sheldrick, 1997).[27] See the Supporting Information for additional details.

Theoretical calculations: Density functional theory has a good track record as far as predicting the electronic structure of neutral and charged oligothiophene molecules.[28] DFT has been used for the ground-state properties (i.e., optimized geometries, vibrational spectra, etc.) and time-dependent DFT, or TD-DFT, for the estimation of vertical-adiabatic excited-state transitions (i.e., energies and oscillator strengths).[29] The geometries of the relevant excited states were optimized by taking advantage of the restricted single excited configuration interaction approach (CIS) within the Hartree–Fock (HF) approximation, or RCIS/HF, meaning that the single-determinant RHF wavefunction represents the reference determinant in a CIS calculation of excited states.[30]

Most of the calculations were performed with the Gaussian 03 suite of programs.[31] For the DFT calculations, Becke's three-parameter (B3) gradient-corrected exchange functional combined with the Lee–Yang–Parr (LYP) correlation functional was used as implemented in Gaussian 03.[32] The 6-31G** basis set was taken in the DFT and RCIS/HF calculations.[33] Methyl groups were considered instead of hexyl groups in all molecules to reduce the computational cost. No constraints were imposed during the geometry optimizations. In the TD-DFT calculations, an evaluation of at least the 10 lowest-energy vertical electronic excited states was carried out. TD-DFT calculations were performed by using the same functional (B3LYP, UB3LYP for the closed and open shell systems) and basis set (6-31G**). Theoretical Raman spectra were obtained for the optimized ground-state geometries; the harmonic vibrational frequencies and Raman intensities were calculated analytically and numerically, respectively.

Results and Discussion

Absorption spectra: Figure 1 displays the absorption spectra of the target molecules in dichloromethane solution. All the spectra are broad and without defined vibrational structure, which indicates the conformational flexibility of both series of molecules. In all of the oligomer series, substituting a thiophene ring with a pyrrole ring results in blueshifted absorptions (average shift = 11 nm/0.1 eV). A more pronounced blueshift is seen when thiophene is substituted with an *N*-aryl pyrrole (average shift = 20 nm/0.2 eV). On the other hand, the incorporation of hexyl groups at the α-positions promotes a significant optical gap reduction (on the order of 0.07 eV) due the positive inductive or electron-donation effect of these saturated groups.

TD-DFT calculations at the B3LYP/6-31G** level have been carried out for all molecules under investigation. The results indicate that the low-lying absorption in the electronic spectra can be assigned to a HOMO→LUMO transition, which allows us to relate the experimental trends to the energy and topology of these two orbitals defining the

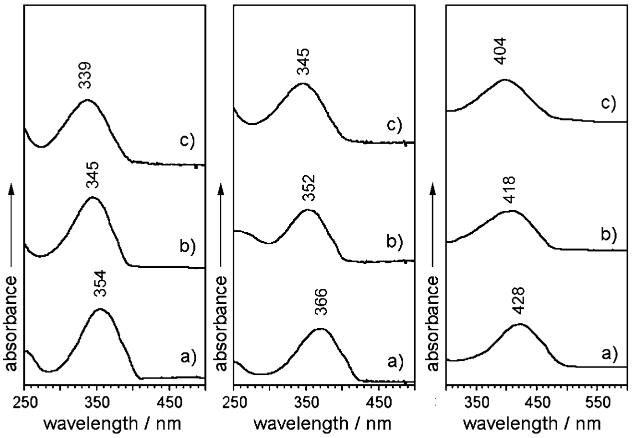

Figure 1. Left: UV/Vis electronic absorption spectra in dichloromethane of a) **3T**, b) **TPT**, and c) **TPT-p(HP)**. Middle: As above for a) **Hex2–3T**, b) **Hex2-TPT**, and c) **Hex2-TPT-p(HP)**. Right: As above for a) **Hex2–5T**, b) **Hex2-TTPTT**, and c) **Hex2-TTPTT-p(HP)**.

energy gap (Figure 2). On the basis of DFT/B3LYP/6-31G** calculations, substituting a thiophene with a pyrrole ring leads to a destabilization of both HOMO and LUMO frontier orbitals. This effect is more pronounced for the LUMO, resulting in an enlargement of the HOMO–LUMO and optical gaps for pyrrole-containing oligomers. This finding can be seen as a consequence of the greater aromatic character of pyrrole relative to thiophene.[34] Due to this increased aromaticity, one would expect some disruption of the conjugation between the two external thiophenes through the pyrrole. This π-electron decoupling has been investigated previously in **TPT**[35] and is also supported by the molecular geometry, more planar in **3T** than in **TPT**, which means greater conjugation in the former (see the section entitled Vibrational Raman spectra), a conjugation dephasing that is insufficient to provoke a donor-to-acceptor charge transfer property.

The higher HOMO/LUMO energies in **TPT** versus **3T** are in line with the fact that polypyrrole presents both a lower ionization potential and a significantly lower electron affinity than polythiophene. For example, the LUMO orbital in **TPT** relative to **3T** is destabilized significantly by 0.51 eV (0.29 eV for the HOMO). This feature is also seen in the case of **TPT-p(PH)**, the HOMO and LUMO of which are also displaced to higher energies relative to **TPT**.

The increase of the chain length, either **Hex2–3T**→**Hex2–5T**, **Hex2-TPT**→**Hex2-TTPTT**, or **Hex2-TPT-p(HP)**→**Hex2-TTPTT-p(HP)**, always produces a destabilization of the HOMO and stabilization of the LUMO as expected from the increase in conjugation in larger linearly connected molecules that overall causes reduction of the HOMO–LUMO and optical gaps.

Fluorescence spectra and lifetimes: Figure 3 compares the absorption and emission spectra of the oligomers. Contrary to the absorption spectra, the emission profiles display a vibronic structure independent of the molecular length and chemical substitution pattern. This feature is due to the quinoidization and subsequent planarization of the molecular backbone in the first singlet excited state (see Figure 4 for

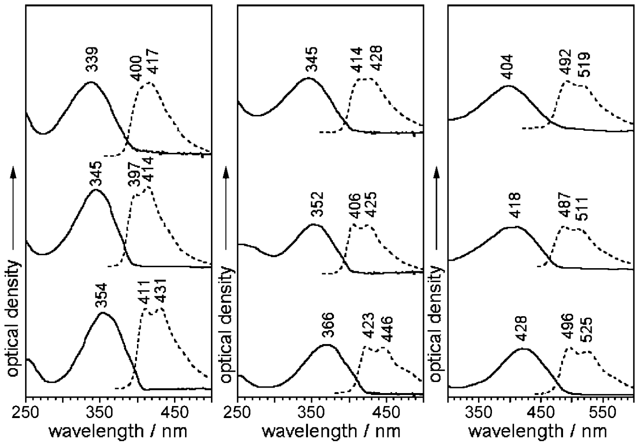

Figure 3. Left: Absorption (——) and emission (-----) spectra in dichloromethane of a) **3T**, b) **TPT**, and c) **TPT-p(HP)**. Middle: As above for a) **Hex2–3T**, b) **Hex2-TPT**, and c) **Hex2-TPT-p(HP)**. Right: As above for a) **Hex2–5T**, b) **Hex2-TTPTT**, and c) **Hex2-TTPTT-p(HP)**.

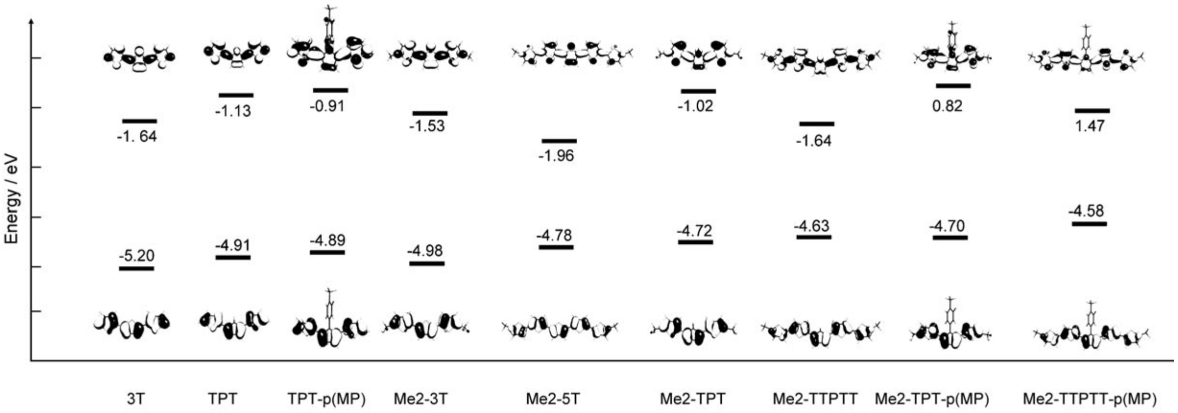

Figure 2. Orbital energies and topologies of the HOMO (top) and LUMO (bottom) according to DFT/B3LYP/6-31G** calculations.

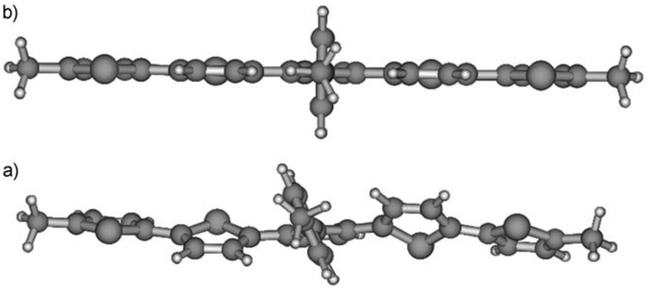

Figure 4. Front view of a) HF/6-31G**-optimized geometry of **Hex2-TTPTT-p(HP)** in the ground electronic state (S_0) and b) HF/RCIS/6-31G**-optimized geometry in the first singlet excited state (S_1).

the optimized geometries in the absorbing S_0 and in the emitting S_1 singlet states), a phenomenon related to the bonding/antibonding pattern between the successive five-membered rings in the HOMO and LUMO orbitals.

The Stokes shifts (evaluated here as the energy difference in eV between the maximum in absorption and the first peak in emission) for the series **3T**→**TPT**→**TPT-p(HP)** evolve as 0.48→0.47→0.56 eV. Two factors are expected to account for these displacements: 1) the overall electronic reorganization upon excitation, which is distinct in the two molecules given the different contribution to the LUMO of N−R compared to S and 2) the planarization of the molecule in the excited state. In **3T** and **TPT**, these two factors appear to be similar (although one has to remain cautious due to the uncertainty in the Stokes shift estimates in spectra with relatively low vibronic resolution). The same happens in **Hex-5T** (0.40 eV) and **Hex-TTPTT** (0.42 eV). For **TPT-p(HP)**, the deviation from planarity in the ground state is larger due to molecular congestion induced by the phenyl group; thus, the vibrational dissipation of energy to reach the excited-state planarization, and consequently the Stokes shift, are greater. Inclusion of hexyl groups at the terminal α-positions minimally alters the Stokes shift (i.e., 0.47 in **TPT** and 0.47 eV in **Hex2-TPT**), in agreement with the π–π* character of the transitions. Finally, chain elongation leads to an evolution from a shift of 0.60 in **Hex2-TPT-p(HP)** to 0.55 eV in **Hex2-TTPTT-p(HP)**, in agreement with the latter being a more conjugated system.

Fluorescence quantum yields were measured for these molecules and are summarized in Table 1 together with the lifetimes and kinetic constants for the radiative and nonradiative processes. Lifetimes are in the nanosecond scale, which indicates the π–π* character of the radiative electronic transitions. Except for **Hex2-TTPTT-(pHP)**, the quantum yields increase when switching from thiophene to pyrrole, in agreement with a less effective heavy-atom effect and intersystem crossing.[36]

Inclusion of an aryl group on the nitrogen atom increases Φ owing to the more distorted system. However, hexyl incorporation negatively affects Φ since the radiationless channels are enhanced. As for chain elongation, Φ increases as commonly found in homogeneous oligothiophenes due to a partial decrease in intersystem crossing in longer oligomers.[37]

Table 1. Photophysical[a] and electrochemical[b] data for oligomers.

Oligomer	λ_{abs}	λ_{em}	Φ_F	τ_F	k_F	k_{NR}	E^o_1	E^o_2
3T	354	411, 431	0.07	0.18	0.39	5.17	1.15[c]	–[d]
TPT	345	397, 414	0.18	0.44	0.41	1.86	0.72[c]	–[d]
TPT-(pHP)	339	400, 417	0.25	0.61	0.41	1.23	0.74[c]	–[d]
Hex2-3T	366	423, 446	0.09	0.20	0.45	4.55	0.92	1.37[d]
Hex2-TPT	352	406, 425	0.10	0.33	0.30	2.73	0.55	1.18[c]
Hex2-TPT-(pHP)	345	414, 428	0.25	0.67	0.37	1.12	0.53	1.14[c]
Hex2-5T	428	496, 525	0.22	0.81	0.27	0.96	0.78	1.01
Hex2-TTPTT	418	487, 511	0.43	1.22	0.35	0.47	0.48	0.89
Hex2-TTPTT-(pHP)	404	492, 519	0.17	1.18	0.14	0.70	0.52	0.86

[a] Wavelength (λ [nm]) of the absorption and emission maxima. Radiative lifetimes (τ_F) in nanoseconds [ns]. Kinetic constants in ns^{-1}. [b] Potentials in Volts [V] vs. Ag/AgCl in 0.1 M $TBAPF_6/CH_2Cl_2$ solution. [c] Irreversible process; E_{pa} value provided. [d] Additional oxidation processes not investigated.

Electrochemical data: Figure 5 displays the cyclic voltammograms of the molecules and Table 1 also summarizes the redox potentials. Stable and reversible oxidations are observed only for the hexyl-capped molecules since the noncapped oligomers undergo radical oligomerization/polymerization. The hexyl-capped compounds display reversible one-electron oxidations generating the radical cation species. The electrochemical formation of these monooxidized species is significantly displaced to lower potentials on going from **Hex2–3T** to the pyrrole-containing oligomers. Within the pyrrole trimers, the oxidation potential of **Hex2-TPT-p(HP)** is 20 mV lower than that of **Hex2-TPT**. It is possible to relate these one-electron oxidation potentials with the absolute HOMO energies according to Koopmans' theorem.[38] For the series **Me2–3T**→**Me2-TPT**→**Me2-TPT-p(HP)**, the HOMO evolves as −4.98→−4.72→−4.70 eV, in good agreement with the trend in the measured potentials of 0.92→0.55→0.53 V. It is pertinent to mention that in nonconjugated amine and thio compounds, the nitrogen-containing compounds always show easier oxidations, a chemical feature exported to the pyrrole and thiophene derivatives, which means that oxidation potentials are not only dictated by the π-valence electrons. This would explain that a more aromatic **TPT** compound shows more accessible oxidations than the more conjugated **3T**. The oxidation potentials to generate some of the dications also deviate from the behavior expected simply from the π-valence electrons, as we will see next.

On going from trimers to pentamers, the first oxidation potentials decrease at the same time that a second reversible one-electron oxidation wave appears due to the formation

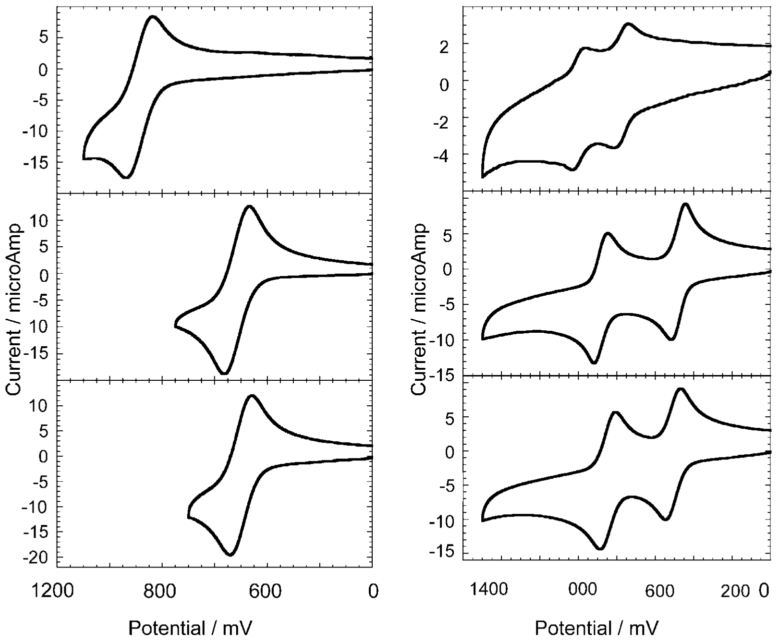

Figure 5. Left: Cyclic voltammograms for **Hex$_2$-3T** (top), **Hex$_2$-TPT** (middle) and **Hex$_2$-TPT-(pHP)** (bottom). Right: Cyclic voltammograms for **Hex$_2$-5T** (top), **Hex$_2$-TTPTT** (middle), and **Hex$_2$-TTPTT-(pHP)** (bottom).

of a dication state. These two processes are again more energetically accessible in the pyrrole pentamers than in **Hex2–5T**. However, the inclusion of the hexyl-phenyl group in **Hex2-TTPTT-p(HP)** has a rather different influence in the formation of this bipolaron-like state: whereas in the radical cations it promotes a stabilization effect (i.e. from [**Hex2-TTPTT**]$^{\cdot+}$ to [**Hex2-TTPTT-p(HP)**]$^{\cdot+}$), the aryl group destabilizes the second electron extraction by 40 mV from [**Hex2-TTPTT**]$^{2+}$ to [**Hex2-TTPTT-p(HP)**]$^{2+}$ (this is also seen in the irreversible oxidation of the trimer to the dication). A tentative explanation could be that the more demanding effect of the doubly charged molecule over the nitrogen atom results in an exceeding electrodeficient situation in N that competes with the σ-electron inductive effect towards the aryl group.

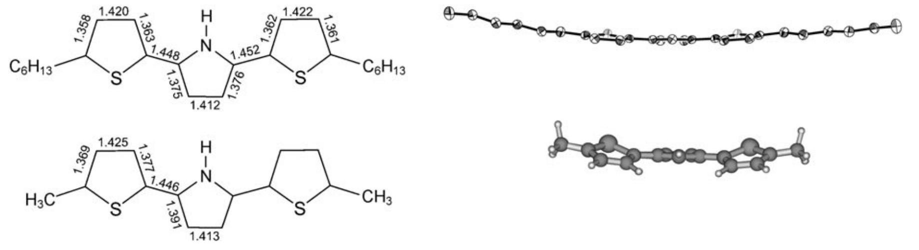

Figure 6. Comparison between the experimental X-ray diffraction molecular structure (top) and the DFT/B3LYP/6-31G**-optimized structure (bottom) for **Hex2-TPT** (**Me2-TPT** in the calculations; distances in Å).

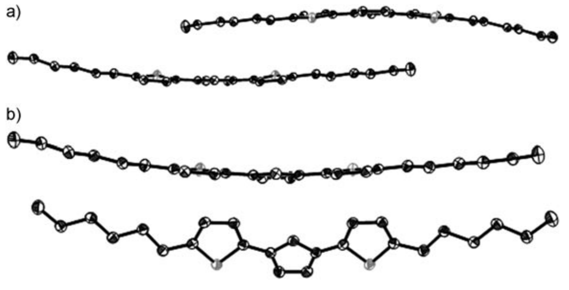

Figure 7. Packing in **Hex2-TPT**: View of the interaction of the hexyl chain with aromatic backbone between two molecules that are in parallel planes (top) and a view of the edge-to-face interaction between molecules (bottom).

Solid-state properties: The crystal structure of **Hex2-TPT** has been resolved by X-ray diffraction of a crystal grown from a CH_2Cl_2/hexane solution. Noteworthy is the fact that the crystal structure of **Hex2–3T** has not been reported yet.

Figure 6 illustrates the deviation from planarity of the three-ring system in both the experimental and calculated structures. In the experimental structure, the pyrrole ring is somewhat out of plane from the thiophene rings. A least-squares plane made from the pyrrole ring is at an angle of 8.9° to a least-squares plane made from the thiophene rings. This feature is also present in the structure predicted by the DFT/B3LYP/6-31G** calculation. Figure 6 also compares the experimental and theoretical C–C bond distances; the results are consistent with the tendency of the DFT methodology to provide somewhat too long C–C bond lengths in conjugated molecules, though in general the agreement is good. The packing in **Hex2-TPT** (Figure 7) consists of layers of molecules in parallel planes that overlap with the hexyl groups of each molecule over the ring systems of the next. These pairs of interacting molecules then repeat down the layer in a ladder motif. This layer of interacting molecules in parallel planes then interacts with a symmetry-related layer on each side in an edge-to-face fashion. As a result, π-stacking is not present in this structure.

Vibrational Raman spectra: Figure 8 compares the FT-Raman spectrum of **Hex2-TPT** with the theoretical Raman

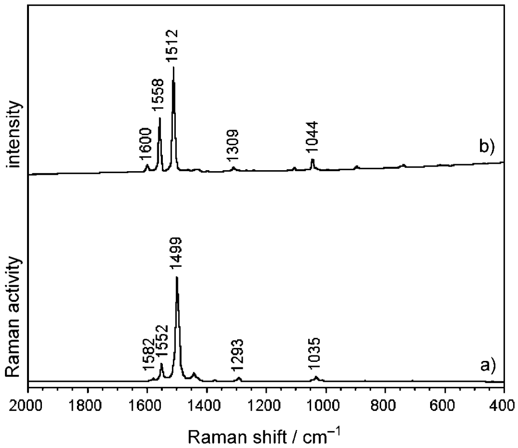

Figure 8. Comparison between a) the theoretical DFT/B3LYP/6-31G** spectrum of **Me2-TPT** and b) the experimental 1064 nm FT-Raman spectrum of **Hex2-TPT**.

spectrum of **Me2-TPT**. There is good agreement between the experimental and theoretical data, which allows for an accurate assignment of the main Raman lines to normal modes, and an understanding of the changes in the spectra on the basis of the molecular structures. The most intense experimental Raman bands at 1558 and 1512 cm^{-1} are reproduced at 1552 and 1499 cm^{-1}, respectively, and can be assigned to the antisymmetric C=C stretching vibration of the external thiophene rings and to the symmetric C=C stretching vibration of these rings, which is more delocalized toward the central pyrrole ring.[39]

Figure 9 displays the FT-Raman spectra of the trimer compounds, whereas Scheme 3 shows the DFT/B3LYP/6-31G** optimized geometries. Substitution of S by N−R produces a net displacement of the intense Raman bands to higher frequencies, an effect that can be accounted for as follows: 1) the more aromatic character of the nitrogen-based five-membered ring reinforces the five-membered structure, which thus requires more energy to carry out the ring stretches and 2) the larger distortion of the molecular backbone in the pyrrole derivative, which negatively affects the molecular conjugation (we recall that an increase in conjugation is accompanied by a frequency downshift[39]). On the other hand, frequencies in **TPT-p(HP)** are slightly higher relative to **TPT**, which can be understood on the basis of the larger oligomer distortion caused by this bulky group (i.e., 12° in Scheme 3).

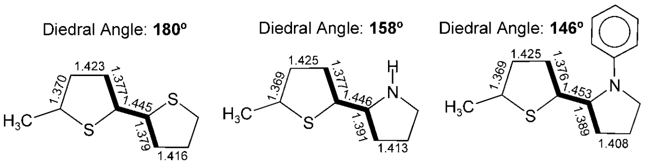

Scheme 3. DFT/B3LYP/6-31G**-optimized geometries of the trimer compounds (methyl instead of hexyls). Only half the molecule is shown.

The Raman spectra also reflect the inclusion of the hexyl groups at the α-positions. It is observed that the main Raman frequencies move to higher values with α,α'-alkylation. The case of the frequency behaviour is more complex than the optical spectral trend (which can be accounted for on the basis of a positive inductive effect alone) since there are two possible effects acting over the vibrational force field: 1) the same inductive effect that alters the geometries and the frequencies (i.e., upshift) and 2) a mechanical effect since the movement of the external C=C stretches is significantly modified by attaching the more heavy hexyl groups (relative to hydrogen in the uncapped molecules).[40]

Figure 10 compares the FT-Raman spectra of the pentamers, in which two main trends are deduced: 1) the main Raman lines are displaced to lower frequencies with respect to the homologous trimers, by −11 cm^{-1} from **Hex2–3T**→**Hex2–5T**, −11 cm^{-1} from **Hex2-TPT**→**Hex2-TTPTT**, and −15 cm^{-1} from **Hex2-TPT-p(HP)** →**Hex2-TTPTT-p(HP)**. This feature is due to the better conjugation in a larger π-electron system, a phenomenon reflected in the calculated CC bond lengths and dihedral angles in **Hex2-TPT** and in **Hex2-TTPTT** that display a slight quinodization and planarization, respectively, in the pentamer due to conjugation (see Figure S1 in the Supporting Information).

The introduction of the aryl groups connected to the nitrogen atom induces a shortening of the C=C pyrrole bond

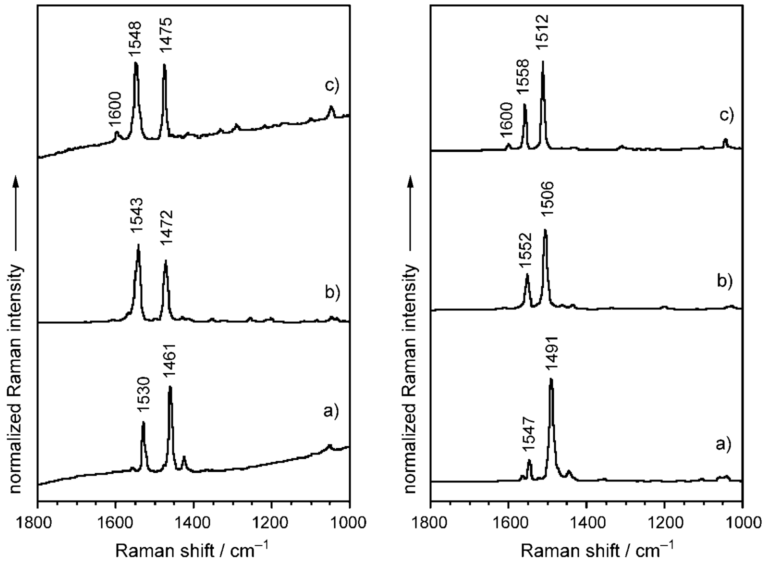

Figure 9. Left: Solid state 1064 FT-Raman spectra of a) **3T**, b) **TPT**, and c) **TPT-p(HP)**. Right: Solid state 1064 FT-Raman spectra of a) **Hex2–3T**, b) **Hex2-TPT**, and c) **Hex2-TPT-p(HP)**.

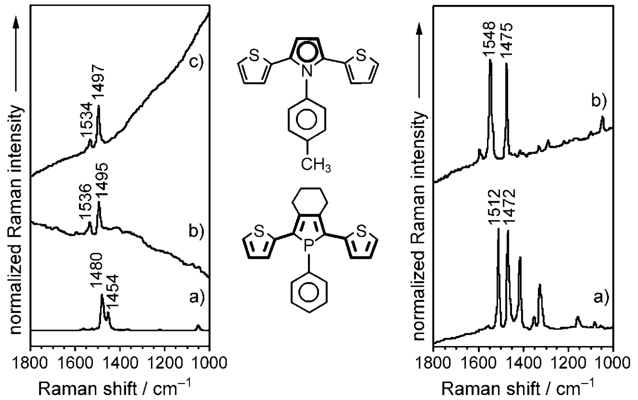

Figure 10. Left: Solid state 1064 FT-Raman spectra of a) **Hex2–5T**, b) **Hex2-TTPTT**, and c) **Hex2-TTPTT-p(HP)**. Right: As above for a) a thiophene–phosphole trimer (see insert) and b) **TPT-p(HP)**. The insert shows the chemical structures denoting in bold the case of cyclic and linear conjugation discussed in the text.

lengths (Scheme 3) from 1.393 in **Hex2-TTPTT** to 1.391 Å in **Hex2-TTPTT-p(HP)** and also in the thiophene bond lengths due to the molecular distortion and π-electron delocalization disruption, all together inducing the frequency upshift.

We conclude this section by addressing the aromaticity versus conjugation question and providing another perspective related to the substitution of the nitrogen atom with phosphorus. The nonaromatic character of phosphole provides us with the opportunity of comparing the impact in the vibrational spectra of the replacement of an aromatic five-membered ring (i.e., pyrrole) with a nonaromatic one (i.e., phosphole).[41] The spectra of the thiophene–phosphole trimer in Figure 10 (see the insert for the complete chemical structure) and that of **TPT-p(HP)** are compared.[41] Interestingly, the Raman line most associated with the stretching movement of the central ring appears at similar frequencies but reflects two competing effects with three characteristics: 1) in the case of **TPT-p(HP)**, this frequency is related to its aromatic character, which is also referred to as ring or cyclic conjugation;[41] 2) in the case of the phosphole derivative, the frequency position is due to the increased diene character (i.e., double bonds strengthened, nonaromaticity) of the phosphole moiety; and 3) to distinguish the two effects in the spectra, the key bands are those at a higher frequency due to the thiophenes: in the case of pyrrole, linear inter-ring conjugation is impeded and the thiophenes are "isolated" showing the Raman band at 1548 cm^{-1}. Instead, for the phosphole system, the diene character (resulting from its nonaromaticity) facilitates interthiophene electronic communication causing the typical frequency downshift of the Raman bands, down to 1512 cm^{-1} in the thiophene–phosphole trimer, which indicates more effective linear interannular conjugation.[42]

Oxidized species: This section is devoted to the spectroscopic properties of the oxidized species generated in the electrochemical processes, which would correspond to the main charge carriers associated with hole mobility in such molecular-based semiconductors. Investigation of the optical and vibrational properties of these oxidized species will allow us to find new insights on the molecular and electronic structures of the charged species, and to study in the cations the changes imparted by thiophene→pyrrole substitution and chain elongation. Chemical oxidation with $FeCl_3$ has been carried out in dichloromethane up to the radical cation and the UV/Vis–NIR spectra are shown in Figure 11.

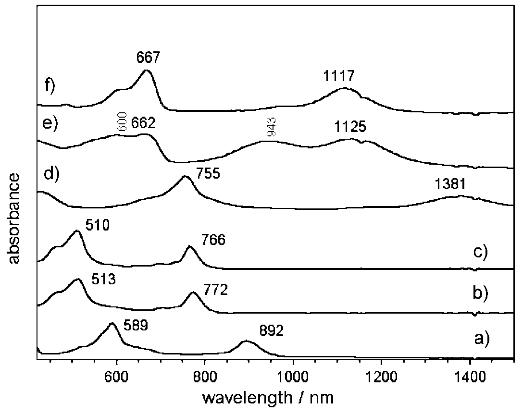

Figure 11. UV/Vis-NIR spectra of the radical cations of a) **Hex2–3T**, b) **Hex2-TPT**, c) **Hex2-TPT-p(HP)**, d) **Hex2–5T**, e) **Hex2-TTPTT**, and f) **Hex2-TTPTT-p(HP)** obtained after oxidation with $FeCl_3$ in CH_2Cl_2.

The spectra of the radical cations show the typical two-band pattern corresponding to the intragap transitions generated after one-electron extraction from the HOMO (SOMO→LUMO and HOMO→SOMO transitions). On the basis of previous works on these oxidized species,[43] we assign the absorption band at lowest energies, for example, at 772 nm in **Hex2-TPT**, to the HOMO→SOMO one-electron transition, and the intense absorption at 513 nm in **Hex2-TPT** to the SOMO→LUMO one-electron excitation. Both bands are of π–π* character and polarized along the main molecular axis defined by the alternating C=C/C−C bond sequence, thus resulting in intense electronic absorptions the wavelength position of which strongly depends on the conjugation extension or efficiency. Again, as in the neutral molecules, the S→N−R replacement in the trimer and pentamer series produces a blueshift of these two absorptions. The lesser contributions from the strong electron-donating effect of sulfur, much more accentuated in the case of the electron-deficient cations relative to nitrogen, causes the blueshift in the mixed oligomers. The displacement in the two thienyl–pyrrole compounds is very small, which is in contrast with the behavior of the neutral molecules. Oxidation causes the quinoidization of the conjugated path and its planarization thus minimizing the distorting effect of the phenyl group attached to the nitrogen atoms.

There are a couple of distinctive features in the absorption spectrum of the **Hex2-TTPTT** radical cation at 600 and 943 nm, both displaced to the blue with respect to the main absorptions at 662 and 1125 nm. These blueshifted bands are due to the π-dimer species formed by through-space π-bonding with the two radical cations situated in a parallel, face-to-face configuration.[44] These species have been well characterized in homogeneous oligothiophenes and are interesting species to address the question of aggregation and intermolecular charge migration in crystals and solid stacks of π-conjugated molecules. In the trimers, no evidence of the formation of π-dimers is observed; this is likely due to the presence of the hexyl groups, which hinders a close interaction between the π-clouds, and to the low polarity of the solvent. No clear bands associated to π-dimers are recorded in **Hex2–5T**, which highlights, for this particular issue, the effect of the inclusion of the pyrrole ring. Owing to the requirement of close contact between the conjugated chains the existence of the hexyl–aryl groups in **Hex2-TTPTT-p(HP)** clearly limits the formation of these species due to steric congestion.

The quinoidal sequence in these oxidized conjugated oligomers can also be investigated with Raman spectroscopy. To this end, Figure 12 shows the Raman spectra, as a representative example, of **Hex2-TPT-p(HP)** in its neutral and radical cation states. The neutral bands in dichloromethane at 1558 and 1505 cm^{-1} evolve to lower frequencies at 1539 and 1411 cm^{-1} in the oxidized species. Following the correlation and vibrational description above, these two bands correspond to ring CC stretching modes located at the terminal thiophenes and in the central pyrrole, respectively. The frequency downshift is due to the ring relaxation caused by quinoidization, which reinforces the inter-ring C–C bonds at the expense of the C=C ring bonds. The $-94\,cm^{-1}$ displacement of the pyrrole band indicates that the oxidation affects mainly the center of the molecules and the effect relaxes toward the two thiophene ends in agreement with the role played by the pyrrole group in the electrochemical and UV/Vis–NIR data described above.

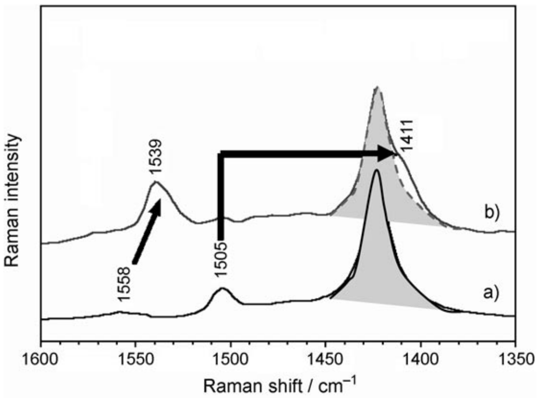

Figure 12. 1064 nm FT-Raman spectra of the neutral (a) and radical cation (b) of **Hex2-TPT-p(HP)**. The solvent band is denoted in grey.

Typical downshifts of 40–60 cm^{-1} are observed in the Raman spectra of homogeneous oligothiophenes upon radical cation formation[45] in contrast with the ≈100 cm^{-1} shift here (i.e., 1505→1411 cm^{-1}) revealing the strong skeletal quinoidization of the CC conjugated chain (most of the extracted electron is released from the C=C/C–C path) to balance the lower electron-donating effect of nitrogen relative to sulfur.

Conclusion

The investigation of thiophene–pyrrole mixed oligomers and the comparison of their properties to those of the analogous oligothiophenes had been scarcely explored. In this work, we have synthesized a new family of pyrrole–thiophene oligomers with different numbers of conjugation units and with different lateral substitutions of the main conjugated backbone, either with hexyl groups (better processability and solid-state properties) or hexyl–phenyl groups (chemical robustness and stability). We have presented a thorough study of their electronic and molecular properties to better understand the role of a more aromatic ring (i.e., pyrrole) in connection with moderate aromatic rings (i.e., thiophenes). In this context, a series of optical (absorption and emission), electrochemical, solid-state, and vibrational studies have been used to provide the physicochemical data required for the discussion of their electro-optical features. The pyrrole inclusion improves both the oxidation capacity and the luminescence properties relative to their homogeneous oligothiophenes. On the other hand, the addition of hexyl and hexyl–phenyl groups might improve the processability and chemical stability, two key requirements for the successful implementation in useful devices. The inclusion of five-membered rings of a different nature causes the molecular π-conjugated backbone to be slightly distorted, whereas conserving good redox and luminescence responses. Overall, this paper sheds light on the potential of mixed thiophene–pyrrole oligomers for use in organic electronics.

Acknowledgements

The present work was supported in part by the Dirección General de Enseñanza Superior (DGES, MEC, Spain) through research project CTQ2006-14987-C02-01 and CT2007-65683. The authors are also indebted to Junta de Andalucía for the project FQM1678/2006. J.C. is grateful to the MEC of Spain for I3 professorship. M.M.O is indebted to the MEC for a predoctoral fellowship. T.M.P. and J.H.M. acknowledge the Morris Academic Partnership Program funded by the University of Minnesota, Morris (UMM) Dean's Office. T.M.P. acknowledges UMM Faculty Research Enhancement Funds supported by the University of Minnesota Office of the Vice President for Research and the UMM Division of Science and Mathematics for financial assistance. K.A.M. acknowledges the University of Minnesota X-ray lab in the Department of Chemistry. K.M.S. acknowledges the University of Minnesota Undergraduate Research Opportunities Program. D.A.S.F. and J.L.B. acknowledge primary support from the MRSEC Program of the National Science Foundation under Award DMR-0819885.

[1] See, for example: a) A. Mishra, C.-Q. Ma, P. Baüerle, *Chem. Rev.* **2009**, *109*, 1141; J. Roncali, *Chem. Rev.* **1997**, *97*, 173; b) D. Fichou, *J. Mater. Chem.* **2000**, *10*, 571; c) Y. Shirota, *J. Mater. Chem.* **2000**, *10*, 1; d) U. Mitschke, P. Baüerle, *J. Mater. Chem.* **2000**, *10*, 1471; e) See the issue of *Chem. Mater.* **2004**, *16*(23); f) A. Facchetti, *Mater. Today* **2007**, *10*, 28; g) J. L. Brédas, J. P. Calbert, D. A. da Silva Filho, J. Cornil, *Proc. Natl. Acad. Sci. USA* **2002**, *99*, 5804.

[2] For example: J. Anthony, *Chem. Rev.* **2006**, *106*, 5028.

[3] For example: I. F. Perepichka, D. F. Perepichka in *Handbook of Thiophene-Based Materials: Applications in Organic Electronics and Photonics*, Wiley, New York, **2009**.

[4] X. Zhang, A. P. Cote, A. J. Matzger, *J. Am. Chem. Soc.* **2005**, *127*, 10502; X. C. Li, H. Sirringhaus, F. Garnier, A. B. Holmes, S. C. Moratti, N. Feeder, W. Clegg, S. J. Teat, R. H. Friend, *J. Am. Chem. Soc.* **1998**, *120*, 2206.

[5] T. Izumi, S. Kobashi, K. Takimiya, Y. Aso, T. Otsubo, *J. Am. Chem. Soc.* **2003**, *125*, 5286; Y. Ie, A. Han, T. Otsubo, Y. Aso, *Chem. Commun.* **2009**, 3020.

[6] Y. Kunugi, K. Takimiya, K. Yamane, K. Yamashita, Y. Aso, T. Otsubo, *Chem. Mater.* **2003**, *15*, 6; K. Takimiya, Y. Konda, H. Ebata, N. Niihara, T. Otsubo, *J. Org. Chem.* **2005**, *70*, 10569; T. Izawa, E. Miyazaki, K. Takimiya, *Chem. Mater.* **2009**, *21*, 903; T. Yamamoto, K. Takimiya, *J. Am. Chem. Soc.* **2007**, *129*, 2224; A. Patra, Y. H. Wijsboom, S. S. Zade, M. Li, Y. Sheynin, G. Leitus, M. Bendikov, *J. Am. Chem. Soc.* **2008**, *130* , 6734.

[7] F. Effenberger, F. Würthner, *Angew. Chem.* **1993**, *105*, 742; *Angew. Chem. Int. Ed. Engl.* **1993**, *32*, 719; F. Effenberger, F. Würthner, F. Steybe, *J. Org. Chem.* **1995**, *60*, 2082; S. Ellinger, U. Ziener, U. Thewalt, K. Landfester, M. Möller, *Chem. Mater.* **2007**, *19*, 1070; T. M. Pappenfus, J. D. Raff, E. J. Hukkanen, J. R. Burney, J. Casado, S. M. Drew, L. L. Miller, K. R. Mann, *J. Org. Chem.* **2002**, *67*, 6015; S. R. González, J. Casado, J. T. López Navarrete, R. Blanco, J. L. Segura, *J. Phys. Chem. A* **2008**, *112*, 6732; J. Casado, T. M. Pappenfus, L. L. Miller, K. R. Mann, E. Ortí, P. M. Viruela, R. Pou-Amérigo, *J. Am. Chem. Soc.* **2003**, *125*, 2524; J. Casado, M. C. Ruiz Delgado, M. C. Rey Merchán, V. Hernández, J. T. López Navarrete, T. M. Pappenfus, N. Williams, W. J. Stegner, J. J. Johnson, B. A. Edlund, D. A. Janzen, K. R. Mann, J. Orduna, B. Villacampa, *Chem. Eur. J.* **2006**, *12*, 5458; S. Mohapatra, B. T. Holmes, C. R. Newman, C. F. Prendergast, C. D. Frisbie, M. D. Ward, *Adv. Funct. Mater.* **2004**, *14*, 605.

[8] S. E. Fritz, S. Mohapatra, B. T. Holmes, A. M. Anderson, C. F. Prendergast, C. D. Frisbie, M. D. Ward, M. F. Toney, *Chem. Mater.* **2007**, *19*, 1355; Y. Nicolas, P. Blanchard, J. Roncali, M. Allain, N. Mercier, A. L. Deman, J. Tardy, *Org. Lett.* **2005**, *7*, 3513.

[9] a) G. Barbarella, L. Favaretto, G. Sotgiu, M. Zambianchi, V. Fattori, M. Cocchi, F. Cacialli, G. Gigli, R. Cingolani, *Adv. Mater.* **1999**, *11*, 1375; b) G. Barbarella, L. Favaretto, G. Sotgiu, M. Zambianchi, A. Bongini, C. Arbizzani, M. Mastragostino, M. Anni, G. Gigli, R. Cingolani, *J. Am. Chem. Soc.* **2000**, *122*, 11971; c) G. Gigli, O. Inganas, M. Anni, M. De Vittorio, R. Cingolani, G. Barbarella, L. Favaretto, *Appl. Phys. Lett.* **2001**, *78*, 1493; d) D. Pisignano, M. Anni, G. Gigli, R. Cingolani, M. Zavelani-Rossi, G. Lanzani, G. Barbarella, L. Favaretto, *Appl. Phys. Lett.* **2002**, *81*, 3534; e) M. Pasini, S. Destri, W. Porzio, C. Botta, U. Giovanella, *J. Mater. Chem.* **2003**, *13*, 807; f) G. Barbarella, M. Melucci, G. Sotgiu, *Adv. Mater.* **2005**, *17*, 1581; g) G. Ridolfi, N. Camaioni, P. Samori, M. Gazzano, G. Accorsi, N. Armaroli, L. Favaretto, G. Barbarella, *J. Mater. Chem.* **2005**, *15*, 895; h) M. Melucci, P. Frere, M. Allain, E. Levillain, G. Barbarella, J. Roncali, *Tetrahedron* **2007**, *63*, 9774; i) S. Lattante, G. Barbarella, L. Favaretto, G. Gigli, R. Cingolani, M. Anni, *Appl. Phys. Lett.* **2006**, *89*, 051111/1; j) J. Casado, M. Z. Zgierski, P. C. Ewbank, M. W. Burand, D. E. Janzen, K. R. Mann, T. M. Pappenfus, A. Berlin, E. Pérez-Inestrosa, R. P. Ortiz, J. T. López Navarrete, *J. Am. Chem. Soc.* **2006**, *128*, 10134; k) T. M. Pappenfus, J. H. Melby, B. B. Hansen, D. M. Sumption, S. A. Hubers, D. A. Janzen, P. C. Ewbank, K. A. McGee, M. W. Burand, K. R. Mann, *Org. Lett.* **2007**, *9*, 3721; l) Y. Suzuki, T. Okamoto, A. Wakamiya, S. Yamaguchi, *Org. Lett.* **2008**, *10*, 3393; m) M. C. Suh, B. Jiang, T. D. Tilley, *Angew. Chem.* **2000**, *112*, 2992; *Angew. Chem. Int. Ed.* **2000**, *39*, 2870; n) E. Amir, S. Rozen, *Angew. Chem.* **2005**, *117*, 7540; *Angew. Chem. Int. Ed.* **2005**, *44*, 7374.

[10] J. Chisaka, M. Lu, S. Nagamatsu, M. Chikamatsu, Y. Yoshida, M. Goto, R. Azumi, M. Yamashita, K. Yase, *Chem. Mater.* **2007**, *19*, 2694; C. D. Dimitrakopoulos, P. R. L. Malenfant, *Adv. Mater.* **2002**, *14*, 99; J. A. Letizia, A. Facchetti, C. L. Stern, M. A. Ratner, T. J. Marks, *J. Am. Chem. Soc.* **2005**, *127*, 13476; T. Siegrist, C. Kloc, R. A. Laudise, H. E. Katz, R. C. Haddon, *Adv. Mater.* **1998**, *10*, 379; G. Horowitz, M. E. Hajlaoui, *Adv. Mater.* **2000**, *12*, 1046; T. M. Pappenfus, R. J. Chesterfield, C. D. Frisbie, K. R. Mann, J. Casado, J. D. Raff, L. L. Miller, *J. Am. Chem. Soc.* **2002**, *124*, 4184; A. Facchetti, M.-H. Yoon, C. L. Stern, G. R. Hutchinson, M. A. Ratner, T. J. Marks, *J. Am. Chem. Soc.* **2004**, *126*, 13480.

[11] S. Martina, A. D. Schlüter, *Macromolecules* **1992**, *25*, 3607; S. Martina, V. Enkelmann, A. D. Schlüter, *Synth. Met.* **1992**, *51*, 299; L. Groenendaal, H. W. I. Peerlings, J. L. J. Van Dongen, E. E. Havinga, J. A. J. M. Vekermans, E. W. Meijer, *Macromolecules* **1995**, *28*, 116; G. Zotti, S. Martina, G. Wegner, A. D. Schlüter, *Adv. Mater.* **1992**, *4*, 798; C. P. Andrieux, P. Hapiot, P. Audebert, L. Guyard, D. A. Nguyen, L. Grenendaal, E. W. Meijer, *Chem. Mater.* **1997**, *9*, 723; J. P. Ferraris, R. G. Andrus, D. C. Hrncir, *J. Chem. Soc. Chem. Commun.* **1989**, 1318; R. E. Niziurski-Mann, C. Scordilis-Kelley, T. L. Liu, M. P. Cava, R. T. Carlin, *J. Am. Chem. Soc.* **1993**, *115*, 887; R. E. Niziurski-Mann, M. P. Cava, *Adv. Mater.* **1993**, *5*, 547; J. P. Parakka, J. A. Jeevarajan, A. S. Jeevarajan, L. D. Kispert, M. P. Cava, *Adv. Mater.* **1996**, *8*, 54.

[12] J. A. E. H. van Haare, L. Groenendaal, H. W. I. Peerlings, E. E. Havinga, J. A. J. M. Vekemans, R. A. J. Janssen, E. W. Meijer, *Chem. Mater.* **1995**, *7*, 1984; J. A. E. H. van Haare, L. Groenendaal, E. E. Havinga, R. A. J. Janssen, E. W. Meijer, *Angew. Chem.* **1996**, *108*, 696; *Angew. Chem. Int. Ed. Engl.* **1996**, *35*, 638.

[13] M. Yu, G. D. Pantos, J. S. Sessler, B. L. Pagenkopf, *Org. Lett.* **2004**, *6*, 1057; T. M. Pappenfus, B. J. Hermanson, T. J. Helland, G. G. W. Lee, S. M. Drew, K. R. Mann, K. A. McGee, S. C. Rasmussen, *Org. Lett.* **2008**, *10*, 1553.

[14] a) J. L. Sessler, A. Aguilar, D. Sánchez-García, D. Seidel, T. Kohler, F. Arp, V. M. Lynch, *Org. Lett.* **2005**, *7*, 1887; b) M. Fujii, T. Nishinaga, M. Iyoda, *Tetrahedron Lett.* **2009**, *50*, 555.

[15] For a recent review: S. Allard, M. Forster, B. Souharce, H. Thiem, U. Scherf, *Angew. Chem.* **2008**, *120*, 4138; *Angew. Chem. Int. Ed.* **2008**, *47*, 4070.

[16] For a recent review: I. F. Perepichka, D. F. Perepichka, H. Meng, F. Wudl, *Adv. Mater.* **2005**, *17*, 2281.

[17] C.-Q. Ma, E. Mena-Osteritz, T. Debaerdemaeker, M. M. Wienk, R. A. J. Janssen, P. Bauerle, *Angew. Chem.* **2007**, *119*, 1709; *Angew. Chem. Int. Ed.* **2007**, *46*, 1679; N. Neghisi, K. Takimiya, T. Otsubo, Y. Harima, Y. Aso, *Chem. Lett.* **2004**, *33*, 654; M. K. R. Fischer, I. López-Duarte, M. M. Wienk, M. V. Martínez-Díaz, R. A. J. Janssen, P. Bauerle, T. Torres, *J. Am. Chem. Soc.* **2009**, *131*, 8669; S. Roquet, A. Cravino, P. Leriche, O. Alévêque, P. Frère, J. Roncali, *J. Am. Chem. Soc.* **2006**, *128*, 3459.

[18] V. Navarro-Fuster, E. M. Calzado, M. G. Ramirez, P. G. Boj, J. T. Henssler, A. J. Matzger, V. Hernández, J. T. López Navarrete, M. A. Díaz-García, *J. Mater. Chem.* **2009**, *19*, 6556; R. Hibino, M. Nagawa, S. Hotta, M. Ichikawa, T. Koyama, Y. Taniguchi, *Adv. Mater.* **2002**, *14*, 119; M. Ichikawa, R. Hibino, M. Inoue, T. Haritani, S. Hotta, K. Araki, T. Koyama, Y. Taniguchi, *Adv. Mater.* **2005**, *17*, 2073; K. Shimizu, D. Hoshino, S. Hotta, *Appl. Phys. Lett.* **2003**, *83*, 4494.

[19] G. Barbarella, L. Favaretto, G. Sotgiu, M. Zambianchi, L. Antolini, O. Pudova, A. Bongini, *J. Org. Chem.* **1998**, *63*, 5497.

[20] Stille coupling was performed as outlined in the following: J. A. Merlo, C. R. Newman, C. P. Gerlach, T. W. Kelley, D. V. Muyres, S. E. Fritz, M. F. Toney, C. D. Frisbie, *J. Am. Chem. Soc.* **2005**, *127*, 3997.

[21] L. F. Schweiger, K. S. Ryder, D. G. Morris, A. Glidle, J. M. Cooper, *J. Mater. Chem.* **2000**, *10*, 107.

[22] P. E. Just, K. I. Chane-Ching, P. C. Lacaze, *Tetrahedron* **2002**, *58*, 3467.

[23] L.-H. Chen, C.-Y. Wang, T.-M. H. Luo, *Heterocycles* **1994**, *38*, 1393; K. Ogura, R. Zhao, H. Yanai, K. Maeda, R. Tozawa, S. Matsumoto, M. Akazome, *Bull. Chem. Soc. Jpn.* **2002**, *75*, 2359.
[24] W. Li, H. E. Katz, A. J. Lovinger, J. G. Laquindanum, *Chem. Mater.* **1999**, *11*, 458.
[25] An empirical correction for absorption anisotropy, R. Blessing, *Acta Crystallogr. Sect. A* **1995**, *51*, 33.
[26] SAINT+ V6.45, Bruker Analytical X-Ray Systems, Madison, WI, **2003**.
[27] SHELXTL V6.14, Bruker Analytical X-Ray Systems, Madison, WI, **2000**.
[28] D. A. da Silva Filho, V. Coropceanu, D. Fichou, N. E. Gruhn, T. G. Bill, J. Gierschner, J. Cornil, J. L. Brédas, *Philos. Trans. R. Soc.* **2007**, *365*, 1435.
[29] P. J. Stephens, F. J. Devlin, F. C. F. Chabalowski, M. J. Frisch, *J. Phys. Chem.* **1994**, *98*, 11623; J. J. Novoa, C. Sosa, *J. Phys. Chem.* **1995**, *99*, 15837; E. Casida, C. Jamorski, K. C. Casida, D. R. Salahub, *J. Chem. Phys.* **1998**, *108*, 4439; R. E. Stratmann, G. E. Scuseria, M. J. Frisch, *J. Chem. Phys.* **1998**, *109*, 8218.
[30] J. B. Foresman, M. Head-Gordon, J. A. Pople, M. J. Frish, *J. Phys. Chem.* **1992**, *96*, 135.
[31] Gaussian 03, Revision C.02, M. J. Frisch, G. W. Trucks, H. B. Schlegel, G. E. Scuseria, M. A. Robb, J. R. Cheeseman, J. A. Montgomery, Jr., T. Vreven, K. N. Kudin, J. C. Burant, J. M. Millam, S. S. Iyengar, J. Tomasi, V. Barone, B. Mennucci, M. Cossi, G. Scalmani, N. Rega, G. A. Petersson, H. Nakatsuji, M. Hada, M. Ehara, K. Toyota, R. Fukuda, J. Hasegawa, M. Ishida, T. Nakajima, Y. Honda, O. Kitao, H. Nakai, M. Klene, X. Li, J. E. Knox, H. P. Hratchian, J. B. Cross, V. Bakken, C. Adamo, J. Jaramillo, R. Gomperts, R. E. Stratmann, O. Yazyev, A. J. Austin, R. Cammi, C. Pomelli, J. W. Ochterski, P. Y. Ayala, K. Morokuma, G. A. Voth, P. Salvador, J. J. Dannenberg, V. G. Zakrzewski, S. Dapprich, A. D. Daniels, M. C. Strain, O. Farkas, D. K. Malick, A. D. Rabuck, K. Raghavachari, J. B. Foresman, J. V. Ortiz, Q. Cui, A. G. Baboul, S. Clifford, J. Cioslowski, B. B. Stefanov, G. Liu, A. Liashenko, P. Piskorz, I. Komaromi, R. L. Martin, D. J. Fox, T. Keith, M. A. Al-Laham, C. Y. Peng, A. Nanayakkara, M. Challacombe, P. M. W. Gill, B. Johnson, W. Chen, M. W. Wong, C. Gonzalez, J. A. Pople, Gaussian Inc., Wallingford CT, **2004**.
[32] A. D. Becke, *J. Chem. Phys.* **1993**, *98*, 1372.
[33] M. M. Francl, W. J. Pietro, W. J. Hehre, J. S. Binkley, M. S. Gordon, D. J. Defrees, J. A. Pople, *J. Chem. Phys.* **1982**, *77*, 3654.
[34] B. S. Jursic, *THEOCHEM* **1998**, *454*, 105.
[35] J. Seixas de Melo, F. Elisei, R. S. Becker, *J. Chem. Phys.* **2002**, *117*, 4428.
[36] D. Grebner, M. Helbig, S. Rentsch, *J. Phys.Chem.* **1995**, *99*, 16991; J. Seixas de Melo, L. M. Silva, M. Kuroda, *J. Chem. Phys.* **2001**, *115*, 5625; H. D. Burrows, J. Seixas de Melo, C. Serpa, L. G. Arnaut, I. Hamblett, S. Navaratnam, *J. Chem. Phys.* **2001**, *115*, 9601.
[37] R. S. Becker, J. Seixas de Melo, A. L. Maçanita, F. Elisei, *J. Phys.-Chem.* **1996**, *100*, 18683.
[38] T. Koopmans, *Physica* **1934**, *1*, 104.
[39] V. Hernández, J. Casado, F. J. Ramírez, G. Zotti, S. Hotta, J. T. López Navarrete, *J. Chem. Phys.* **1996**, *104*, 9271.
[40] J. Casado, H. E. Katz, V. Hernández, J. T. López Navarrete, *J. Phys. Chem. B* **2002**, *106*, 2488.
[41] C. Hay, M. Hissler, C. Fischmeister, J. Rault-Berthelot, L. Toupet, L. Nyulászi, R. Réau, *Chem. Eur. J.* **2001**, *7*, 4222; C. Hay, D. Le Vilain, V. Deborde, L. Toupet, R. Réau, *Chem. Commun.* **1999**, 345; C. Hay, C. Fischmeister, M. Hissler, L. Toupet, R. Réau, *Angew. Chem.* **2000**, *112*, 1882; *Angew. Chem. Int. Ed.* **2000**, *39*, 1812; C. Hay, C. Fave, M. Hissler, J. Rault-Berthelot, R. Réau, *Org. Lett.* **2003**, *5*, 3467; C. Fave, M. Hissler, K. Sénéchal, I. Ledoux, J. Zyss, R. Réau, *Chem. Commun.* **2002**, 1674.
[42] J. Casado, R. Réau, J. T. López Navarrete, *Chem. Eur. J.* **2006**, *12*, 3759.
[43] J. Casado, M. Z. Zgierski, R. G. Hicks, D. J. T. Myles, P. M. Viruela, E. Ortí, M. C. Ruiz Delgado, V. Hernández, J. T. López Navarrete, *J. Phys. Chem. A* **2005**, *109*, 11275.
[44] L. L. Miller, K. R. Mann, *Acc. Chem. Res.* **1996**, *29*, 417; D. Yamazaki, T. Nishinaga, T. Tanino, K. Komatsu, *J. Am. Chem. Soc.* **2006**, *128*, 14470; J. A. E. H. van Haare, E. E. Havinga, J. L. J. van Dogen, R. A. J. Janssen, J. Cornil, J. L. Brédas, *Chem. Eur. J.* **1998**, *4*, 1509; T. Sakai, T. Satou, T. Kaikawa, K. Takimiya, T. Otsubo, Y. Aso, *J. Am. Chem. Soc.* **2005**, *127*, 8082; J. Casado, K. Takimiya, T. Otsubo, F. J. Ramírez, J. J. Quirante, R. Ponce Ortiz, S. R. González, M. Moreno Oliva, J. T. López Navarrete, *J. Am. Chem. Soc.* **2008**, *130*, 14028.
[45] J. Casado, V. Hernández, S. Hotta, J. T. López Navarrete, *J. Chem. Phys.* **1998**, *109*, 10419; J. Casado, V. Hernández, S. Hotta, J. T. López Navarrete, *Adv. Mater.* **1998**, *10*, 1458; J. Casado, L. L. Miller, K. R. Mann, T. M. Pappenfus, Y. Kanemitsu, E. Orti, P. M. Viruela, P. Pou-Amerigo, V. Hernández, J. T. López Navarrete, *J. Phys. Chem. B* **2002**, *106*, 3872; J. Casado, L. L. Miller, K. R. Mann, T. M. Pappenfus, V. Hernández, J. T. López Navarrete, *J. Phys. Chem. B* **2002**, *106*, 3597.

Received: January 19, 2010